Electronic structure and properties of strained polymers: 2. Rigid-rod PBI, PBO and PBZT

Scott G. Wierschke
Department of Chemistry USAF Academy, CO 80840, USA

and James R. Shoemaker and Peter D. Haaland
Air Force Institute of Technology, Wright-Patterson Air Force Base, OH 45433, USA

and Ruth Pachter* and W. Wade Adams†
Wright Laboratory, Materials Directorate, WL/MLPJ, Wright-Patterson Air Force Base, OH 45433, USA
(Received 2 April 1991; revised 3 September 1991; accepted 23 September 1991)

A theoretical study of single-chain moduli employing the molecular-orbital semi-empirical AM1 (Austin model 1) approach is presented for the poly(*p*-phenylene benzobisimidazole) (PBI), poly(*p*-phenylene benzobisoxazole) (PBO) and poly(*p*-phenylene benzobisthiazole) (PBZT) rigid-rod polymers. This computational study is important for comparisons of mechanical properties for the series of related polymers. An analysis of molecular deformation on tension and compression of these rigid-rod polymers offers an insight into tensile and compressive processes at the molecular level, allowing their relative ordering by theoretical tensile and/or compressive strength and moduli. Furthermore, an examination of the electronic structures of these molecular systems containing various hetero atoms provides insight into the charge distribution and bond order changes on the application of strain. This approach will be useful for the relative prediction of the properties of polymers that have not yet been synthesized.

(Keywords: mechanical properties; molecular structure; rigid-rod polymers; poly(*p*-phenylene benzobisimidazole); poly(*p*-phenylene benzobisoxazole); poly(*p*-phenylene benzobisthiazole); strain; theoretical modulus)

INTRODUCTION

Most organic polymers, owing to their long and flexible chain structures, assume random molecular conformations and, barring crystallization, random intermolecular orientations in the solid form and in solution. There is a class of organic polymers that, owing to their more rigid molecular structure, tend to aggregate and orient themselves into much more ordered (liquid-crystalline) solutions, films and fibres than typical flexible polymers. These are termed *ordered polymers*[1] and have shown the highest fibre tensile properties of any organic material except graphite[2]. The invention by DuPont chemists of the solution spinning of liquid-crystalline acid solutions of the stiff-chain poly(*p*-phenylene terephthalamide (Kevlar™) opened that field of extremely high-performance organic fibres[3]. Studies of the rigid-rod benzazoles, namely poly(*p*-phenylene benzobisoxazole) (PBO) and poly(*p*-phenylene benzobisthiazole) (PBZT), have produced fibres with approximately double the tensile properties of Kevlar[2]. These fibres, however, show poor axial compressive strength, the bane of all organic fibres[4]. Only recently have rigid-rod polymers been synthesized of sufficiently high molecular weight to exhibit mechanical properties of commercial interest. Indeed, the ordered polymers studied so far show tensile properties high enough to make them candidates for incorporation into aerospace structures. Reviews of ordered polymers have recently appeared[5,6], and an entire recent Materials Research Society Symposium[7] was directed to that subject.

Computational chemistry provides powerful tools for explaining and predicting chemical and physical phenomena such as organic chemical reactions, the study of protein and other biological systems, and gas-phase chemistry, but there have been relatively few polymer studies using quantum-mechanical techniques. This is primarily due to the molecular size of polymeric systems, which prohibits the computation of a long polymer chain. Thus, smaller model systems have to be employed, the properties of which are then extrapolated to the molecular length of the polymer. The advent of the periodic boundary condition approximation for a single chain repeat unit offers a useful alternative for calculations of large chain systems.

*This work was done while the author held a National Research Council Research Associateship
†To whom correspondence should be addressed

0032-3861/92/163357-12

In an effort to understand the limits to the ultimate mechanical properties achievable with rigid polymeric chains, we have been involved in a continuing research effort to calculate these properties for individual chains. The ultimate axial chain (molecular) modulus is especially important in predicting mechanical properties of a molecular composite, where the rigid-rod molecules reinforce a flexible-chain matrix polymer. Furthermore, the property–molecular structure relationship is examined, so that we can gain insight into the parameters that affect the mechanical properties of these polymer systems. The calculations also offer an insight for molecular design; a figure of merit for fibre processing efficiency; an understanding of the molecular nature of deformation, and prediction of temperature dependence. The purpose of this publication is to study theoretically the tension and compression of single chains of poly(*p*-phenylene benzobisimidazole) (PBI), PBO and PBZT (*Figures 1a–1c*, respectively) rigid rods in an attempt to understand the tensile and compressive phenomena of these systems and to predict the tensile moduli. Although theoretical studies on these individual molecular systems have already been performed[8], no systematic study on the effects of tensile and compressive strain on these polymers and their mechanical properties has yet been reported. Attempts to calculate moduli of polymer crystals have been reported[9], but these methods rely on molecular-mechanics potential energy functions, and do not attempt molecular-orbital calculations.

Cis- and *trans*-PBI rigid rods were first synthesized in 1975 and reported in 1976[10]. The polymer chain is extended and rigid as there are no tetrahedral centres where coiling bond rotations can occur. These rigid rods were synthesized under the assumption that stiff extended-chain molecules would align to provide high strength and modulus. The *cis* and *trans* derivatives do not appear separately since the polymer is made in polyphosphoric acid and all nitrogens are protonated, and a random distribution of *cis* and *trans* derivatives along a chain would occur. However, computationally it is possible to study the two isomers independently and to make observations as to various properties of the two different structures that would not be possible experimentally. The tensile moduli of both *cis*- and *trans*-PBI are calculated in this study and an extensive molecular tensile and compressive analysis is reported and discussed for the *cis* isomer. PBI has not been synthesized in sufficiently high molecular weight for the determination of any of its mechanical properties, since it easily hydrogen bonds and precipitates out of solution[11]; hence no comparison with experiment is attempted.

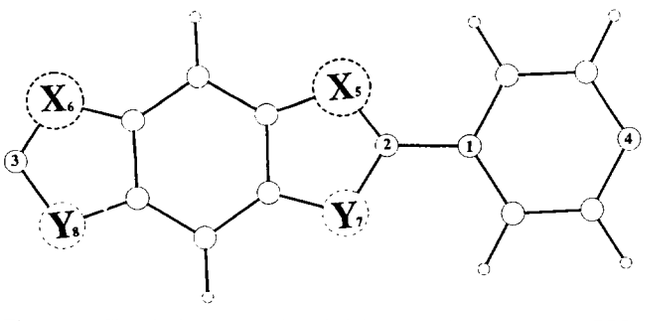

Figure 1 Chemical repeat units of rigid-rod polymers: (a) *cis*-PBI, X = Y = N; (b) *cis*-PBO, X = N and Y = O; (c) *cis*-PBZT, X = N and Y = S; a *trans* derivative implies an exchange of the X and Y hetero atoms in one of the heterocyclic rings

Cis- and *trans*-PBO rigid rods were first synthesized in 1975[12–14]. *Cis*-PBO is under study at present by Dow Chemical and others[7] for use as a high-performance fibre or film, while *trans*-PBO is difficult to synthesize in high molecular weights due to quinone formation in the *p*-hydroxy monomer. A computational study of the theoretical moduli of both *cis*- and *trans*-PBO as undertaken in this investigation provides information on the difference in properties of these isomers and allows a comparison to other rigid rods. *Cis*- and *trans*-PBZT rigid rods, which were first synthesized in 1978[15,16], are the sulphur analogues to *cis*- and *trans*-PBO. Both materials have been studied structurally, and are also of interest in the area of non-linear optics. Model compounds of *cis*- and *trans*-PBZT have also been studied by X-ray crystallography[17], revealing that *cis*-PBZT appears as a bowed, less extended structure than *trans*-PBZT. Theoretical moduli for *cis*- and *trans*-PBZT and the molecular deformations of *trans*-PBZT on the application of tension and compression are calculated in this study, and a comparison of these two structures, and to other rigid rods, is discussed, providing information on the effect of larger hetero atoms, e.g. sulphur, on the tensile and compressive properties of ordered polymers. In addition, an analysis of the charge distribution provides further insight on the effect of different hetero atoms on the electron density and delocalization patterns in the strained polymeric systems of *cis*-PBO, and *cis*- and *trans*-PBZT, which are important in estimating non-linear susceptibilities.

METHODOLOGY

Polymer structure calculations

Polymer structure calculations were performed using the molecular-orbital (MO) approach which invokes the semi-empirical neglect of differential overlap approximation at the modified level AM1 (Austin model 1)[18]. The cluster method[19] was used, which defines a fragment of a polymer chain as one or more repeat units. The position of the atoms of the cluster in a repeat unit are determined by internal coordinates in the usual way, while periodic boundary conditions[20] are used to describe the pseudo-bond between the end atoms of different repeat units, characterized by the translation vector (T_v). In simple cases, the cluster method is essentially identical to the Hückel methodology treatment of cyclic bonding. The minimal cluster length required is determined by the electron delocalization length within the polymer. For most polymers a cluster length of 10 Å is suitable, while a cluster length of 10–20 Å is required for polymers containing π conjugated bonds. A cluster of one repeat unit satisfies this requirement for the PBI, PBO and PBZT polymers. The advantage in using the cluster method is that 'end effects', which are always present in oligomer approximations of polymers, are completely eliminated. This has been demonstrated in previous studies, in which good agreement between calculated polymer heats of formation at the semi-empirical level and experimentally measured properties have been obtained[19,21].

The modulus calculation proceeds in two stages. The equilibrium geometry of the cluster is first calculated by energy minimization using the AM1 Hamiltonian, and

the translation vector is thereafter incrementally increased or decreased, representing molecular tensile or compressive strain. The geometry of the cluster is reoptimized under this constraint, and the heat of formation calculated. Clearly, the heat of formation is higher for the strained geometry than for the equilibrium length. Thus, by optimizing the geometry at a number of different T_v values, the dependence of the heat of formation on molecular tension and compression can be established. The stiffness of the polymer chain, namely the force (spring) 'constant', is given by the second derivative of the heat of formation *versus* strain relation, which, along with the cluster length and polymer unit-cell cross-sectional area, can then be used to calculate polymer chain modulus.

These optimized geometries describe molecular deformations, i.e. bond stretching, angle bending or twisting, as well as changes in the electronic structure, which are monitored as a function of tensile or compressive strain, thus showing how the repeat unit reacts to the input of compressive or tensile force. Using the AM1 Hamiltonian, one can calculate the partitioning of electron density into atomic charges and bond order[22], which offers further insight, for example, with respect to hetero atom changes.

Theoretical tensile modulus

The elastic modulus of a polymer is determined by the ratio of the stress σ (force per unit area) and the strain ε (fractional change in cluster length $\Delta L/L_{eq}$):

$$E = \sigma/\varepsilon = (F/A)/(\Delta L/L_{eq}) = KL_{eq}/A_{eq} \quad (1)$$

where K is the force constant ($K = F/\Delta L$, N m^{-1}) and L_{eq} is the equilibrium length of the polymer obtained from the semi-empirical calculation. The force constant is calculated from the second derivative of the Helmholtz free energy ($= U - TS$; U is the internal energy, T the temperature and S the entropy). In this case (at 0 K) this is derived from the potential energy by the MO method with respect to the strain applied to the translation vector, namely the change in cluster length (ΔL). The temperature dependence of the modulus was recently calculated for PBZT[23]. The change in the heat of formation calculated with the AM1 Hamiltonian is fitted to a third-order polynomial[21]:

$$\Delta H_{ff} = a(\Delta L)^3 + b(\Delta L)^2 + c(\Delta L) + d \quad (2)$$

where b is related to the molecular force constant ($b = K/2$) at equilibrium at 0 K. The analytic second derivative of this potential is then given by:

$$d^2(\Delta H_{ff})/d(\Delta L)^2 = K + 6a(\Delta L) \quad (3)$$

while the first derivative is used for the expression for the stress for a given ΔL:

$$\sigma = (1/A)[c + K\Delta L + 3a(\Delta L)^2] \quad (4)$$

Alternatively, numerical differentiation of the potential curve can be used in order to obtain the force constant. It was found that, within the semi-empirical approximation, the force constants obtained from either a third-order polynomial fit or by the numerical differentiation used in this study agree to within the error of the fitting procedure. The cross-sectional area of the polymer used in equation (1) is either obtained from experimental X-ray diffraction unit cells, or estimated from the polymer density d (g cm^{-3}) by the expression:

$$d = m/V = m/(A_{eq}L_{eq}) = nM_w/(A_{eq}L_{eq}) \quad (5)$$

so that:

$$A_{eq} = M_w/dN_AL_{eq} \quad (6)$$

where A_{eq} is the cross-sectional area of the polymer at its equilibrium length (Å^2); M_w the molecular weight of the cluster (g mol^{-1}), n the number of moles, V the volume and N_A Avogadro's number.

RESULTS AND DISCUSSION

Moduli calculations

A representative modulus calculation is shown in *Figure 2* for *cis*-PBI, where the calculated ΔH_{ff} values are plotted as a function of strain (-15% to 15%) along the polymer axis. Since the AM1 Hamiltonian is parametrized only to reproduce equilibrium molecular properties, the validity of the calculations for strains larger than 5% is questionable. Indeed, this issue is addressed in paper 1 of this series[24]. However, the full range is presented in order to show the calculated predicted behaviour. There are two features in this potential that are of interest. First, there is a sharp discontinuity at a tensile strain of 11%, after which the energy remains essentially constant as a function of strain. At this strain, bond breaking occurs; further separation of the fragments should not change their energy. Secondly, the energy increases linearly with increasing compressive strain beyond 3% compressive strain. The importance of this feature becomes evident when the behaviour of the corresponding force curve in *Figure 2*

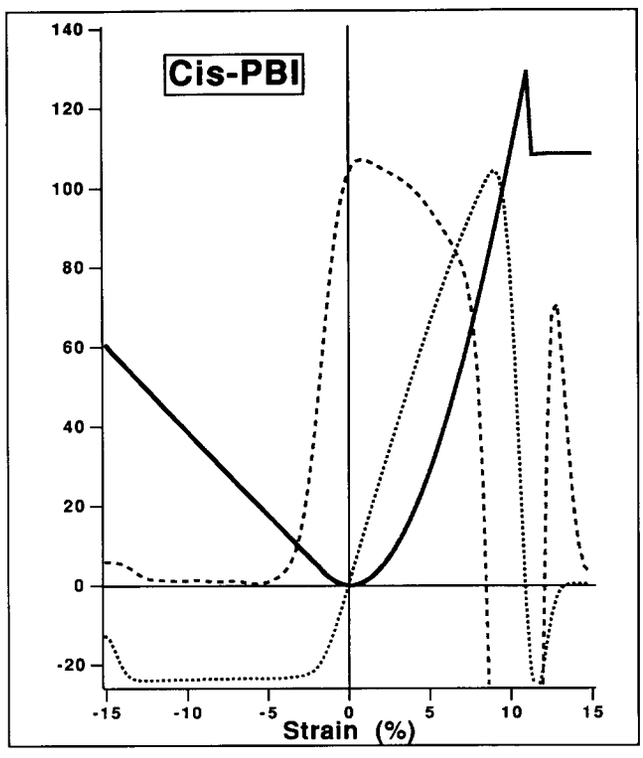

Figure 2 *Cis*-PBI energy (kcal mol^{-1}) vs. strain (%) dependence is shown by the full curve (contains ~110 points). The dotted curve is the corresponding force curve (10^{-10} N), obtained by taking a numerical derivative of the energy curve. The broken curve is the second derivative of the energy potential (N m^{-1})

is examined. In tension, the force curve crosses zero at approximately 11% tensile strain, then becomes negative, and finally rebounds to a positive value. This behaviour is an artifact of the numerical differentiation around the discontinuity in the energy potential and has no physical significance. In compression, the force curve is seen to cross the origin, decrease linearly and remain roughly constant beyond a compressive strain of 2%. The second derivative of the potential energy, namely the stiffness, is also given in *Figure 2*. This compares well to macroscopic stress–strain curves for rigid-rod fibres, for example those of PBO (cf. Figure 28 in ref. 5), to the Raman frequency shift dependence on composite strain[25], and also to the non-linear elasticity of PBZT fibres[26]. The elastic behaviour of real materials is only approximated by a harmonic potential for small values of strain around equilibrium, and hence the second derivative of the *cis*-PBI potential is not a constant. A cubic expression of the potential gives a more realistic description of the strain-dependent stiffness behaviour than a harmonic potential and is both asymmetric and stiffer on compression. The stiffness in *Figure 2* decreases linearly to approximately 7% tensile strain, and then rapidly falls to zero. In compression, the stiffness falls off to zero at about 4% compressive strain and then remains approximately constant, at value zero. The maximum stiffness of *cis*-PBI is found to be 107 N m^{-1}; combined with a cluster length[27] of 12.31 Å and a unit-cell cross-sectional area[27] of 20.9 Å^2, this value translates to a chain modulus magnitude of 630 ± 30 GPa. The modulus of *cis*-PBI is directly proportional to the stiffness curve in *Figure 2*, so that the strain-dependent behaviour of the modulus follows that of stiffness[28].

The overall behaviour for *trans*-PBI described in *Figure 3* is very similar to that of *cis*-PBI. The maximum value of the stiffness of *trans*-PBI is approximately 2%

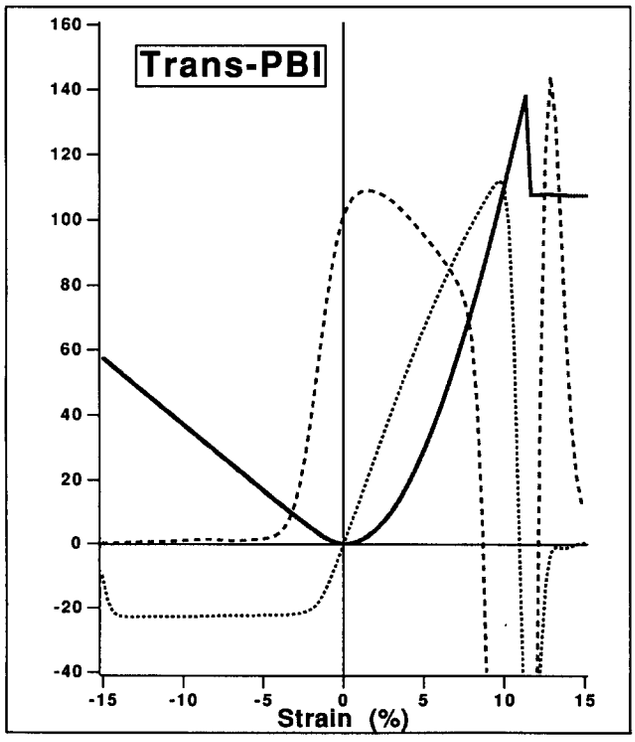

Figure 3 Energy (kcal mol^{-1}) vs. strain (%) dependence for *trans*-PBI; curves description in caption of *Figure 2*

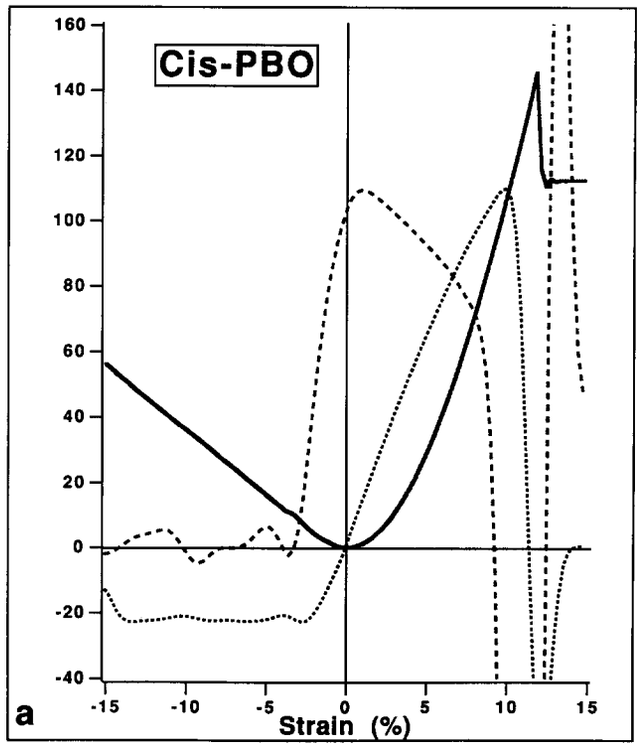

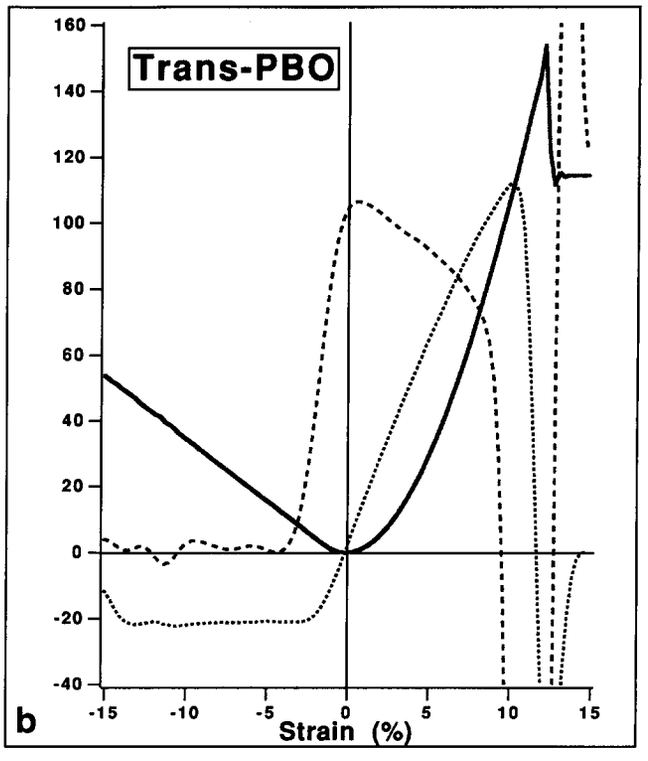

Figure 4 Energy (kcal mol^{-1}) vs. strain (%) dependence: (a) *cis*-PBO and (b) *trans*-PBO; curves description in caption of *Figure 2*

lower than for *cis*-PBI, but this difference is within the overall uncertainty of 5% of the stiffness, which arises from the uncertainty in the numerical differentiation procedure. Similarly, *Figure 4a* shows the energy, force and stiffness curves for *cis*-PBO, while *Figure 4b* relates this information for *trans*-PBO. Once again, the same general behaviour as that seen for PBI is observed. The maximum values of the stiffness of 109 and 107 N m^{-1}, cluster length[27] of 12.30 Å and unit-cell cross-sectional area[27] of 19.2 Å^2 result in chain moduli of 690 ± 30 and

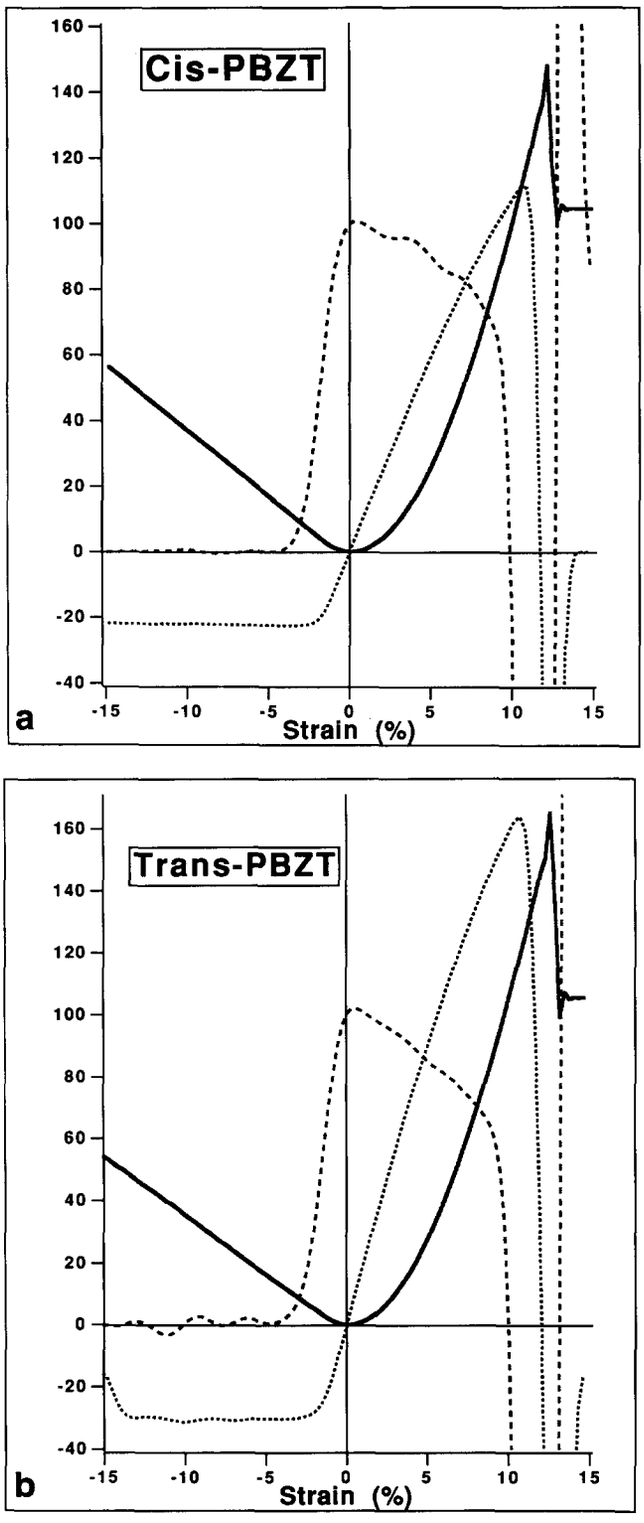

Figure 5 Energy (kcal mol^{-1}) vs. strain (%) dependence: (a) *cis*-PBZT and (b) *trans*-PBZT; curves description in caption of *Figure 2*

680 ± 30 GPa for *cis*-PBO and *trans*-PBO, respectively. The larger modulus calculated for PBO as compared to that of PBI results from PBO's smaller cross-sectional area (higher density). The corresponding curves for *cis*- and *trans*-PBZT are shown in *Figures 5a* and *5b*, respectively, revealing the same behaviour as seen for PBI and PBO. The maximum values of the stiffness are 95 and 101 $N\,m^{-1}$, which with cluster lengths[27] of 12.51 and 12.56 Å and unit-cell cross-sectional areas[27] of 20.68 and 20.60 $Å^2$, result in moduli of 580 ± 30 and 620 ± 30 GPa for *cis*- and *trans*-PBZT, respectively. PBZT shows the largest difference in moduli between the *cis* and *trans* configurations of the rigid rods, which may be due to the distorted geometry[17], resulting from the size difference between the sulphur and nitrogen atoms in the heterocycle moiety.

A comparison of the calculated moduli by AM1 and MNDO (modified neglect of differential overlap)[21], X-ray diffraction measured moduli and mechanically measured moduli is reported in *Table 1*. The Klei and Stewart[21] modulus values have been adjusted to account for the more accurate densities of PBO and PBZT that have become available since their report. The difference between the AM1 and MNDO moduli arises from the inherent differences in the two Hamiltonians. MNDO predicts a minimum energy geometry for PBO and PBZT in which the phenyl and heterocycle rings are perpendicular, while AM1 predicts these rings to be nearly coplanar in PBO, which agrees with experimental structure measurements[8,27]. There are no parameters for sulphur for the AM1 Hamiltonian as yet, so that the PBZT calculations were performed with MNDO parameters for sulphur and AM1 parameters for all other atoms. This results in a minimum energy geometry in which the heterocycle and phenyl rings are at a 40° angle with respect to each other instead of 20–30° (refs 8, 27, 29).

The calculated moduli reported in this paper are systemically higher than the experimentally measured values. This discrepancy may result first from the fact that even under the best conditions real material properties are always limited by deviations from ideal structures. The method presented in this study calculates the modulus of a single ideal polymer chain. If a real polymer solid could be made with perfect lateral order, perfect orientation and no imperfections such as chain ends, lattice defects, etc. (Staudinger's 'continuous crystal' model), its uniaxial modulus would be equal to that of the ideal chain modulus[30]. Consequently, the polymer moduli calculated by this procedure represent the ultimate moduli that can be achieved for a uniaxially oriented material. If two different polymers could be made to satisfy the above three conditions, their mechanical properties would differ only by the difference in their intrinsic chain stiffness, i.e. molecular modulus. The lattice prediction for the deformation process of a stressed polymer chain has been discussed[9] and recently assessed for a polyethylene crystal[31]. The inclusion of intermolecular interactions in these calculations requires, however, the use of the semiclassical molecular-mechanics approach for the calculation of the potential energy rather than the semi-empirical Hartree–Fock Hamiltonian. Moreover, in the case of these rigid-rod topologies, small lateral interactions (i.e. only van der Waals interactions) may be assumed, having a negligible contribution to E.

Table 1 Comparison of AM1, MNDO and experimental moduli (GPa)

Polymer	AM1	MNDO[20]	X-ray[42]	Experimental[42]
Cis-PBO	690	670	475	330
Trans-PBO	680	619	–	–
Cis-PBZT	580	602	–	–
Trans-PBZT	620	528	400	300

Secondly, there has emerged evidence[32] that the semi-empirical calculation of polyethylene and polydiacetylene systematically overpredicts bond stiffness K, and hence will systematically overpredict also the modulus. A comparison of vibrational spectra[33] and force constants derived from semi-empirical AM1 calculations on polyethylene is explored in paper 1 of this series[24]. However, this relationship depends on the deformation mode of the polymer chain; bond extension or compression is only one deformation mode of the polymer. At the present time it is difficult to generalize the magnitude of these overpredictions to polymers other than polyethylene and polydiacetylene. It is, however, important to recognize that semi-empirical calculations of polymer moduli may result in overestimated magnitudes.

Molecular deformation

Although the calculation of ultimate single-chain tensile moduli provides quantitative information on the relative strengths and stiffness of different materials and on those structures that show high mechanical properties, no explanation of the origin of the different properties results. In order to explain the observation that one structure may be stiffer or stronger than another, the structure's response to molecular tension and compression must be examined. A molecular deformation analysis can be performed by examining those bond lengths, bond angles and dihedral angles in a polymer repeat unit that exhibit the largest change with tension or compression. For the rigid-rod polymers reported in this study, five such values are monitored: the length of the heterocyclic moiety, the length of the phenyl moiety, the length of the carbon–carbon bond connecting the two groups, the torsion angle between the heterocyclic and phenyl groups, and an angle defining their coplanarity (or collinearity). This is demonstrated in the *cis*-PBO repeat unit (cf. *Figure 6*): the length of the heterocyclic moiety is the distance between atoms A and B (AB); BC is the carbon–carbon bond length connecting the heterocyclic and phenyl moieties; the phenyl length is represented by the distance between atoms C and D (CD); the torsion angle quantifies the relative orientation around the BC bond; and the angle between atoms A, B and D is a measure of the collinearity of the phenyl and heterocyclic groups. Molecular deformation in other rigid rods is monitored in the same manner with the same lettering scheme. These molecular deformation effects on the molecule's modulus, tensile strength and compressive strength are examined by relating their percentage change (relative to the equilibrium value) to the percentage strain (either compressive or tensile) on the unit as a whole. For example, *Figures 6a* and *6b* show the minimum energy geometries of the *cis*-PBO repeat unit before tensile failure where the bond between atoms B and C breaks, and after compressive failure has occurred, respectively, and for comparison also at equilibrium (*Figures 6c*). Indeed, these are geometric points of interest along the energy *versus* strain curve (*Figure 4*) since they illustrate the cumulative deformation of the molecule from tension to compression.

The variations in the C–C bond length, phenyl and benzimidazole lengths, and the torsion angle, with the strain applied along the polymer axis in the *cis*-PBI cluster are shown in *Figures 7a* and *7b*, respectively. The

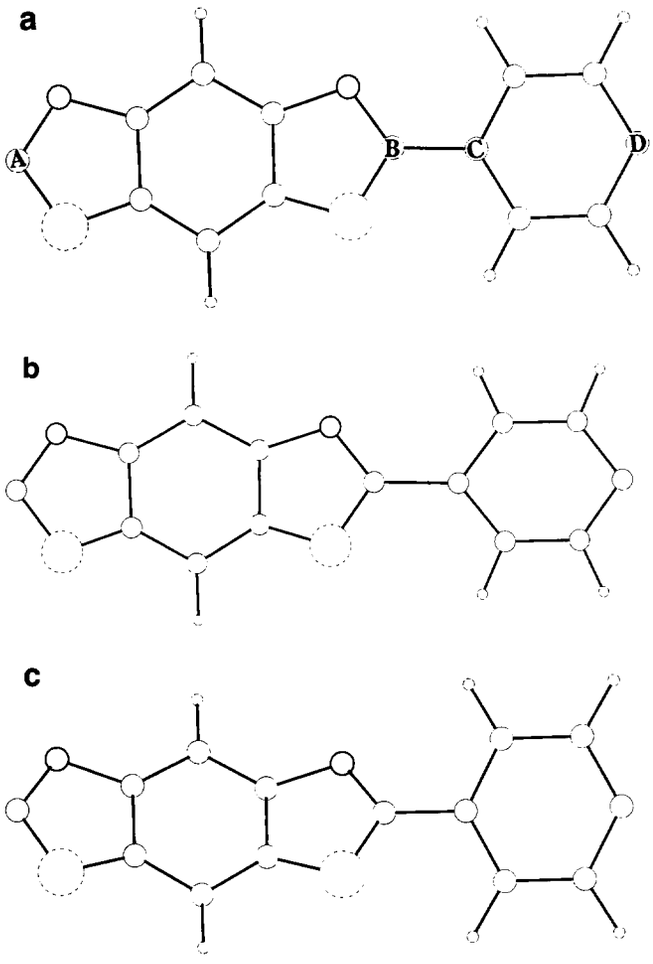

Figure 6 The *cis*-PBO molecular system at two points along the energy vs. strain curve: (a) prior to tensile failure; (b) at compressive failure; and also (c) at equilibrium

lengths are plotted as percentage strain from the equilibrium values. Obviously, as the cluster is stretched, all these three molecular lengths increase. The initial benzimidazole length in *cis*-PBI of 6.576 Å increases by 6.58% to a maximum of 7.009 Å before tensile failure occurs at 11.0% translation vector strain; the initial phenyl length of 2.797 Å increases to 3.182 Å, namely +14.76%, before decreasing at tensile failure; while the C–C bond length of 1.467 Å increases slowly to 1.763 Å, i.e. +19.29%. Thereafter, the C–C bond breaks and the distance increases dramatically (tensile failure). The initial torsion angle of 32° decreases to zero, indicating coplanarity at 4% strain, with the phenyl ring being deformed more than twice as much as that of benzimidazole. The collinearity of the groups does not change with tension. The tensile strain of 11.0% along the polymer axis needed to break the repeat unit proves to be large when compared to the strains that break fibres of rigid-rod materials (approximately 2.0%)[5]. This is not surprising, as the only possible mode of failure in the model studied is bond breakage, while imperfections in bulk materials may cause premature failure.

Variations in C–C length, phenyl length, benzimidazole length, torsion angle and collinearity angle, respectively, on the application of compressive strain to *cis*-PBI are also shown in *Figures 7a* and *7b*. Interestingly, it is calculated that the collinearity angle remains relatively constant (±2°) until −1.93% compressive strain is

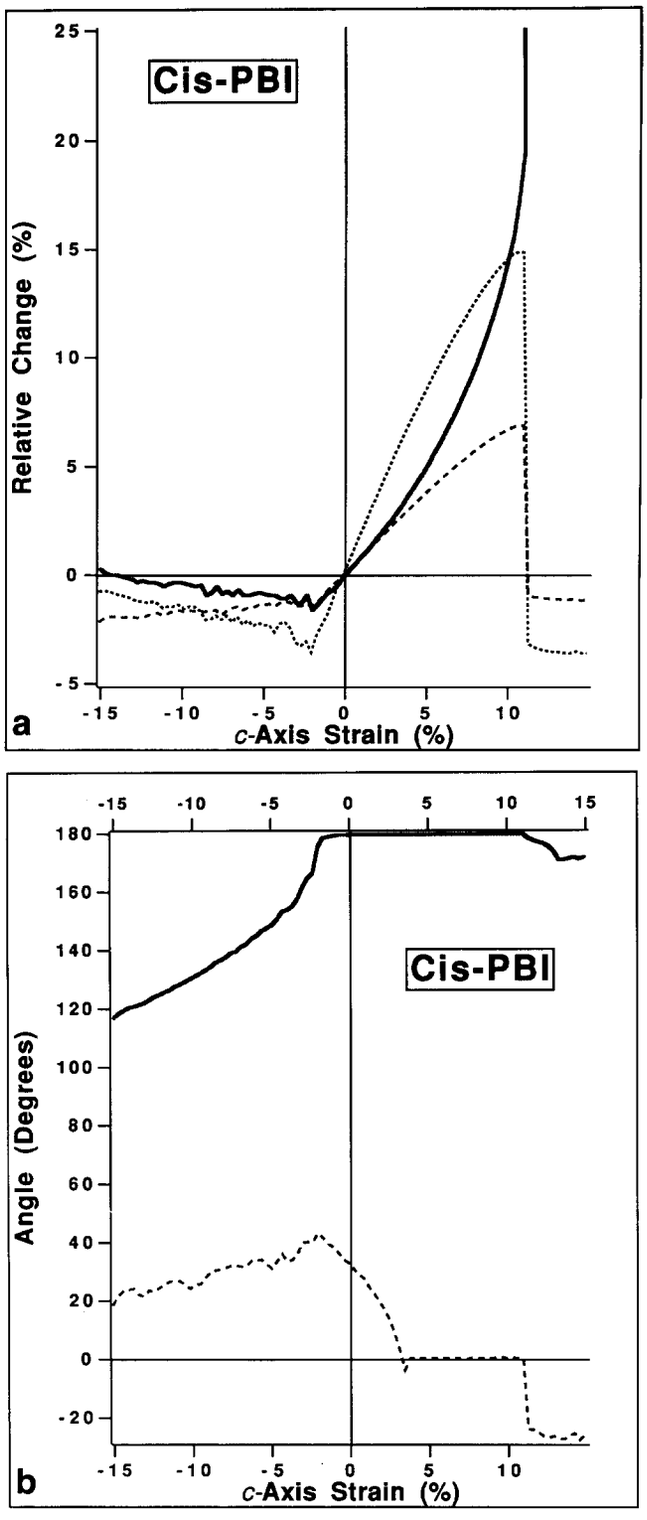

Figure 7 (a) Sub-unit changes (defined in text) (C—C bond length, full curve; phenyl, dotted curve; benzimidazole, broken curve) vs. percentage strain for *cis*-PBI. (b) Bond (full curve) and torsion angle (deg) dependence on strain (%) for *cis*-PBI

applied to the unit, where it increases, so that the unit bends or 'kinks'. The typical mode of compressive failure in rigid-rod polymer fibres is known as 'kinking'[5], so that for our purpose this molecular bending will be equated with compressive failure. As the *cis*-PBI unit is compressed, the C–C bond length shrinks almost linearly to 1.447 Å, or −1.64% from equilibrium, before it increases sharply as the polymer starts to bend. The phenyl group shrinks almost linearly by −3.61% to 2.701 Å before it also increases after compressive failure. The benzimidazole group exhibits a similar behaviour, shirinking to 6.480 Å, or −1.49%, before increasing to −2.0% *cis*-PBI (compressive) strain. The torsion angle increases linearly from 35° to 45° and begins to decrease at the compressive failure point. On the other hand, the torsion angle decreases with tension, possibly as a result of the increase in the C–C bond length, thus decreasing the steric interactions between the phenyl and heterocycle rings. It should be noted that the phenyl ring deforms more than twice as much as benzimidazole, which was also shown for tension. *Figure 7* shows that the compression is absorbed completely by the C–C bond length and the rings until enough energy is supplied to the system to force the molecule to bend, 4.62 kcal mol^{-1} in this case. After bending starts, more compression results in more bending, with the monitored lengths changing back towards their equilibrium value. This collinearity effect is unique to this class of macromolecules.

The tensile and compressive behaviour discussed for PBI is observed in all of the heterocyclic rigid rods studied. In particular, results for *cis*-PBO depicted in *Figures 8a* and *8b* show that in tension the C–C bond stretches by 19.0% before breaking at 11.80% polymer strain, requiring 140 kcal mol^{-1} of energy to bring the *cis*-PBO to tensile failure. The phenyl ring stretches by 14.89% and benzoxazole by 7.60% before they both recoil after failure. The torsion angle of 18.3° at equilibrium decreases to zero at 1.33% unit strain. In compression, the C–C bond shrinks by 1.51%, the phenyl ring by 3.71%, and the benzoxazole by 2.18% before the polymer bends and they begin to lengthen again. The initial torsion angle of 18.3° increases to 32.8° before decreasing on compressive failure. The repeat unit begins to bend, signifying compressive failure, at 2.10% compressive strain; it takes 4.69 kcal mol^{-1} of energy to bring *cis*-PBO to compressive failure[34]. Similarly, *Figures 9a* and *9b* summarize deformation patterns for the *trans*-PBZT molecular system.

The pertinent results for these polymers are collated into *Tables 2a* and *2b* for tension and compression, respectively. An examination of the results in *Table 2a* reveals that in tension all the rigid-rod polymers behave in the same manner. From the start of tension up to tensile failure, the C–C, phenyl and heterocycle lengths stretch in concert, while the phenyl ring is less stiff than the heterocycle in all cases, and deforms more than the heterocycle, twice as much in some cases. Since the phenyl group stretches nearly the same amount in all three rods, the differences in modulus can be attributed to the different stiffness of the heterocyclic moieties. The C–C bond stretches by nearly 20% in most cases, a stiffer heterocycle causing it to be strained more in *cis*-PBI and *cis*-PBO, while a less stiff heterocyclic moiety takes more of the tension itself, leaving the C–C bond less strained in *trans*-PBZT. The torsion angle between the groups decreases to zero on tension. The energy increases with tension until a threshold is reached, E_T, where the C–C bond breaks and the phenyl and heterocyclic groups shrink in recoil. This energy represents the amount of tensile energy needed to break the polymer, and should be proportional to the ultimate tensile strength for the polymer; the higher E_T, the higher the tensile strength.

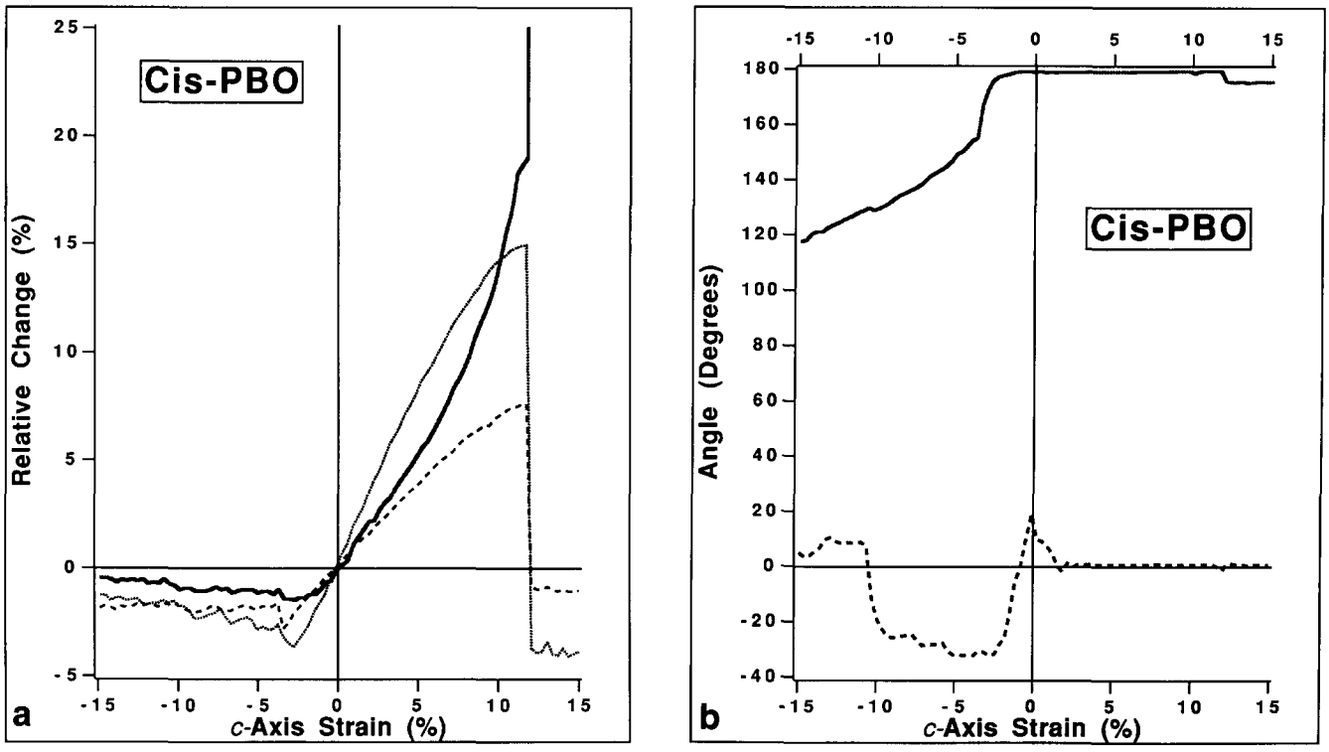

Figure 8 (a) Sub-unit changes (defined in text) vs. percentage strain for *cis*-PBO. (b) Bond and torsion angle (deg) dependence on strain (%) for *cis*-PBO. Description of curves in legend to *Figure 7*

Table 2 Changes in the molecular deformation parameters on the application of tensile and compressive strains

(a) Tensile strain

Polymer	Strain[a] (%)	E_T[b] (kcal mol^{-1})	C–C[c] (%)	Phenyl[d] (%)	Hetero[e] (%)	Torsion[f] (deg)
Cis-PBI	11.20	136.79	20.20	13.77	6.58	35–0
Cis-PBO	11.49	140.22	20.42	13.64	7.21	16–0
Trans-PBZT	12.27	151.28	18.75	13.65	9.20	42–0

(b) Compressive strain

Polymer	Strain[a] (%)	E_C[b] (kcal mol^{-1})	C–C[c] (%)	Phenyl[d] (%)	Hetero[e] (%)	Torsion[f] (deg)
Cis-PBI	1.93	4.62	1.38	3.44	1.46	35–45
Cis-PBO	2.10	4.68	1.25	3.21	1.68	16–28
Trans-PBZT	1.93	4.03	1.24	3.01	1.61	42–56

[a]The percentage strain where tensile or compressive failure occurs
[b]$E_T(E_C)$ are the energy input to bring the polymer to tensile (compressive) failure
[c]Change in C–C bond length
[d]Change in phenyl bond length
[e]Change in hetero bond length
[f]Change in torsion angle

Consequently, the *tensile strength order* is *trans*-PBZT > *cis*-PBO > *cis*-PBI as shown in *Figures 10* and *11*, being nearly opposite to that of modulus.

Table 2b shows that all rigid rods act in a similar way on compression. Initially the C–C bond, phenyl group and the heterocyclic moiety compress, with the phenyl group being, once again, easier to compress, and deforming nearly twice as much as the heterocycle. The torsion angle increases, twisting the two groups farther out of planarity. When enough compressive energy has been input to the molecular system, the molecule begins to bend, the measured lengths increase and the torsion angle decreases. This is termed the point of compressive failure. The energy required to make the polymer bend, E_C, should be proportional to the compressive force required to bring about this failure. The predicted *compressive strength order* of the rigid rods is *cis*-PBO > *cis*-PBI > *trans*-PBZT (cf. *Figures 10* and *11*). However, *cis*-PBO fibres do not exhibit significantly higher compressive strength than those of *trans*-PBZT[5]. It may be inferred that these rigid rods have a molecular instability to kinking, which may initiate the corresponding microscopically observed elastic instability to kinking of the microfibrillar structure[35].

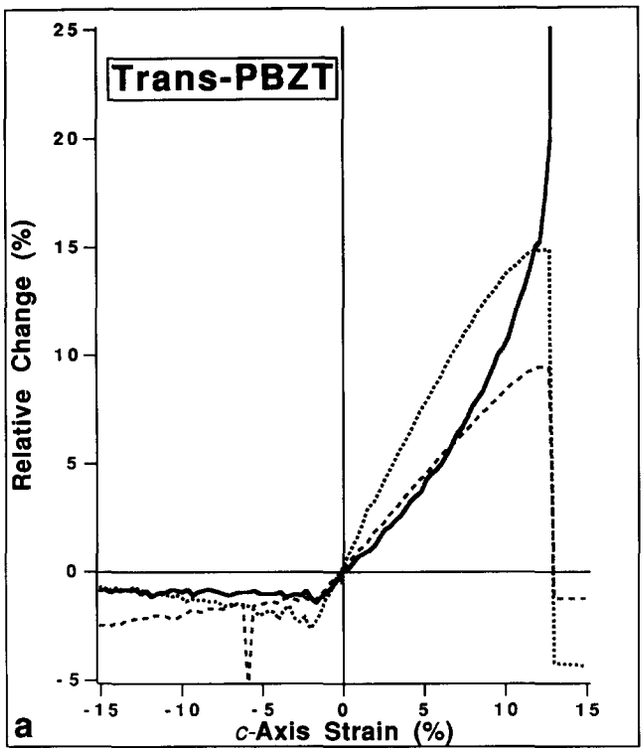

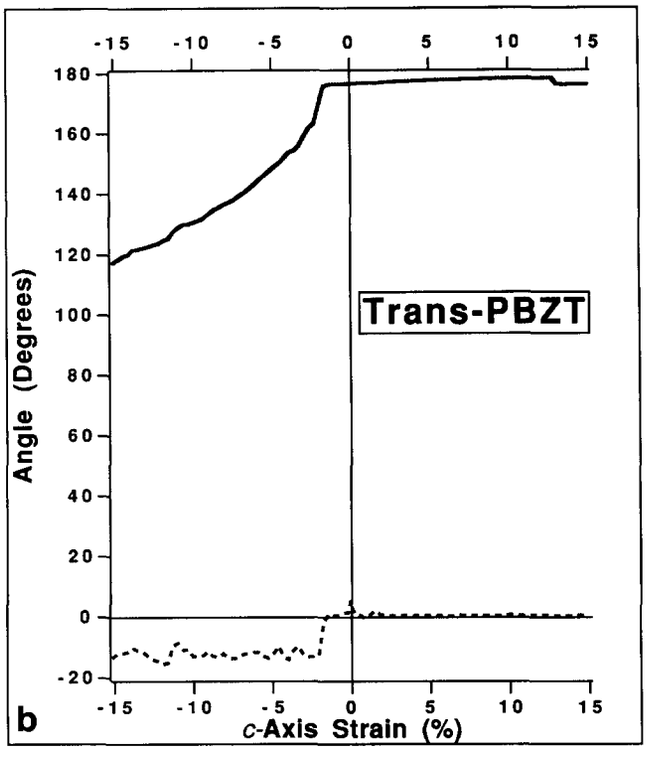

Figure 9 (a) Sub-unit changes (defined in text) vs. percentage strain for *trans*-PBZT. (b) Bond and torsion angle (deg) dependence on strain (%) for *trans*-PBZT. Description of curves in legend to *Figure 7*

Electron distribution analysis

Relatively high magnitudes of the non-resonant third-order optical non-linear susceptibilities, $\chi^{(3)}$, for PBI, PBO and PBZT were measured[36,37] to be as large as 10^{-10} to 10^{-11} esu with a subpicosecond response. The electron density evaluation and the amount of π-electron conjugation in this type of polymer were found to be of importance for an understanding of electronic structure effects on hyperpolarizabilities[38]. Further, the effects of substituents on the hyperpolarizability were even related to the σ Hammett constants[39], which give a measure of the π-resonance effects of various $+R$ and $-R$ substituents. Similarly, a calculation of the electron distribution changes on the application of strain in such a series of related conjugated polymers may serve as the

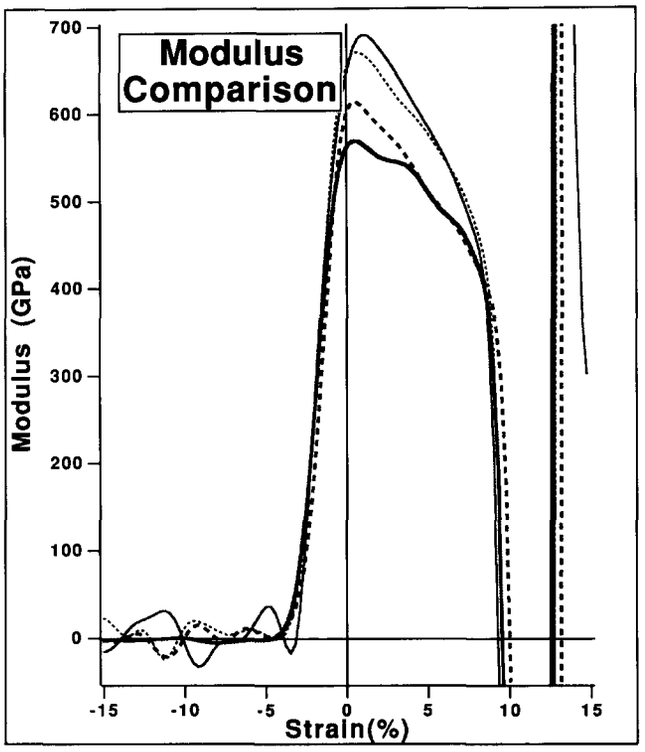

Figure 10 A comparison of modulus (GPa) vs. strain (%) plots for *cis*- and *trans*-PBO (thin and dotted curves, respectively), and *cis*- and *trans*-PBZT (full and broken curves, respectively)

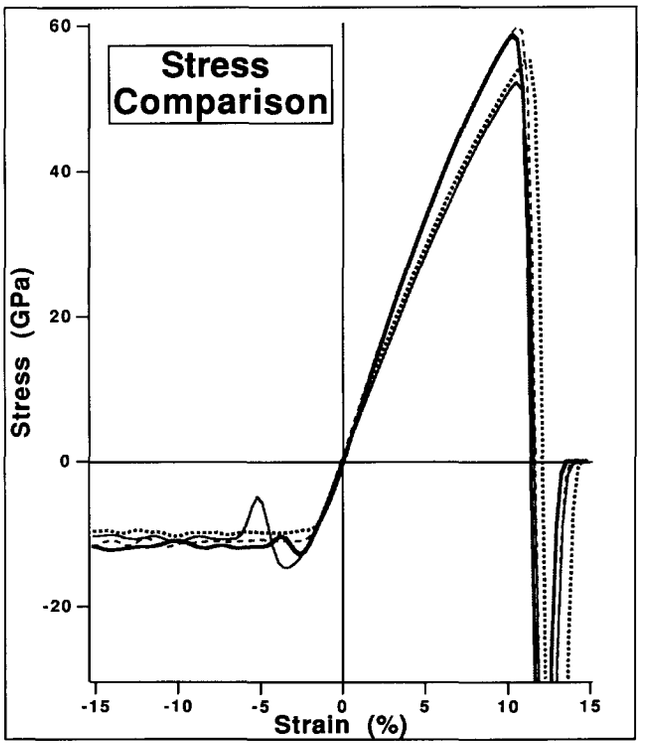

Figure 11 A comparison of stress (GPA) vs. strain (%) plots for *cis*- and *trans*-PBO, and *cis*- and *trans*-PBZT. Description of curves in legend to *Figure 10*

basis for an assessment of their potential for non-linear optics applications in future studies. These changes may not be directly related to the molecular deformation, for example, when changing the hetero atoms in the heterocyclic rings.

The *trans*-PBZT molecular system shows that the largest relative changes in bond order from the equilibrium values occur for the phenyl and heterocyclic linkage (C1–C2 bond; the atom numbering is given in *Figure 1*) and for the C=N bonds in the heterocyclic rings. Changes in the C1–C2 bond order for *trans*-PBZT are depicted in *Figure 12a*, showing a decrease in bond order of up to ~13% at tensile failure, accompanied by an increase in the C=N bond orders of approximately 9%. The decrease in C1–C2 bond order on the application of tensile strain follows a corresponding change in bond length from 1.45 to 1.76 Å, and the C=N bond lengths increase from 1.344 to 1.351 Å, following closely the bond order–bond length relationship outlined recently by Paolini[40]. These variations on tensile strain application are accompanied by a polarization of the charge distribution in the heterocyclic rings, showing changes of up to 55% at C2, C3, N5 and N6 before tensile failure occurs (*Figure 12b*), as well as very large variations at the C1 and C4 atoms (*Figure 12c*). On the application of compressive strain on *trans*-PBZT, the C=N heterocyclic ring bond orders decrease, with a smaller change in charge distribution at C2, C3, N5 and N6. Partial atomic charge changes at C1 and C2 are minimal, accompanied by a small increase in C1–C2 bond order. This small change in bond order corresponds to a decrease in bond length of 0.013 Å, and changes in double bond character in the heterocyclic rings to an increase in bond length to 1.37 Å at −14.3% compressive strain. A slightly different dependence of bond order and atomic charges on the applied strain in polymers of *cis*-PBO emerges, since only the C1–C2 bond order for *cis*-PBO changes by more than 5% on the application of tensile strain. The relation to compressive strain in *cis*-PBO is also somewhat different from that of *trans*-PBZT, in that the C1–C2 bond order increases rather than decreases, with a relatively large change on the immediate application of compression. The same pattern is observed when examining the charge changes at C1 and C2. Bond length dependence on bond order is similar to that of *trans*-PBZT, so that this different behaviour demonstrates a different response of *cis*-PBO to compressive strain. In addition, relatively larger variations in the partial atomic charges at the oxygen atoms are calculated, which may also be due to the substitution of oxygen for sulphur. In order to assess which of the changes in electron density on strain application in *cis*-PBO compared to *trans*-PBZT are related to the atom type in the heterocyclic ring (O vs. S) or to the isomer type (*cis* vs. *trans*), we compared the results to those of *cis*-PBZT. Only the C1–C2 bond order for *cis*-PBZT varies by more than 5% on the application of tensile strain, demonstrating a similar pattern to that of *cis*-PBO. However, it is interesting to point out that on tensile failure the bond order largely decreases in this case contrary to both *trans*-PBZT and *cis*-PBO. This may be explained on the basis of the complete deformation of this part of the polymer unit in this case. The percentage variation in atomic charge shows a similar pattern to that of *trans*-PBZT at both the phenyl and heterocyclic ring atoms.

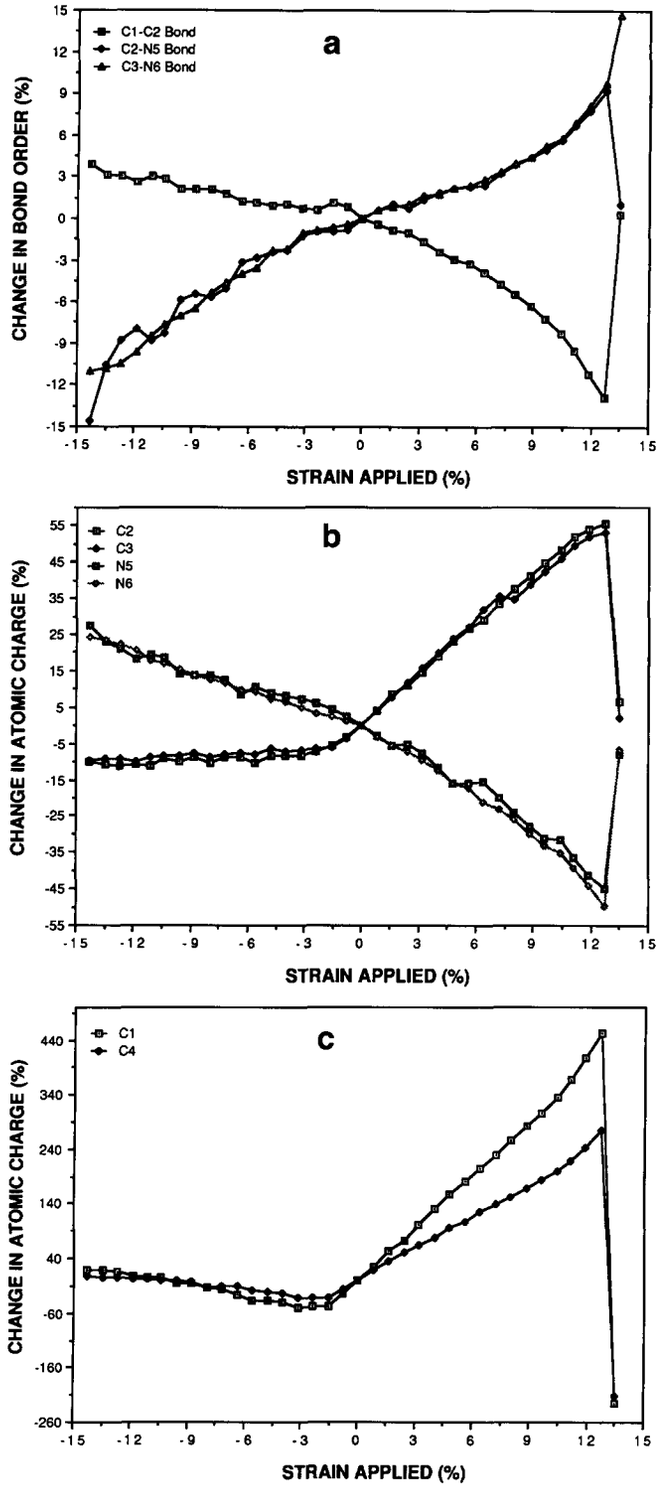

Figure 12 Electron distribution changes (%) as a function of strain for *trans*-PBZT: (a) bond order; (b) atomic charge at C2, C3, N5 and N6 in the heterocyclic rings; (c) atomic charge at C1 and C4

It can be concluded that, while the heterocyclic rings in *trans*-PBZT exhibit much larger localization of atomic charge than in *cis*-PBO on the application of tensile strain owing to the larger stiffness of the heterocyclic rings, *cis*-PBO exhibits the largest relative changes on compression owing to the substitution of oxygen for sulphur. Thus, the *trans* configuration (X vs. Y in *Figure 1*) influences electron distribution on the application of tensile strain, while the type of Y atom (O vs. S) affects it on compression.

Table 3 A comparison of the *cis* and *trans* isomers of PBI, PBO and PBZT[a]

	L_{eq} (Å)	M_w (g mol^{-1})	d (g cm^{-3})	A_{eq} (Å^2)	K (N m^{-1})	TM (GPa)	TS (GPa)	TC (GPa)	ε_T (%)	ε_C (%)	ΔH_T (kcal mol^{-1})	ΔH_C (kcal mol^{-1})
Cis-PBI	12.31	232.24	1.50[b]	20.89	107	630	51.2	10.0	11.0	−2.0	129	5.3
Trans-PBI	12.30	232.24	1.50[b]	20.90	109	640	54.3	9.9	11.3	−2.0	138	4.9
Cis-PBO	12.22	234.21	1.66[c]	19.17	109	690	59.4	9.8	11.8	−1.6	146	3.2
Trans-PBO	12.20	234.21	1.66[c]	19.21	107	680	59.8	10.6	12.0	−2.0	154	4.3
Cis-PBZT	12.51	266.35	1.71[c]	20.68	95	580	52.5	10.3	12.0	−2.2	148	5.2
Trans-PBZT	12.56	266.35	1.71[c]	20.60	101	620	55.0	9.4	12.6	−1.7	165	4.0

[a] L_{eq} and A_{eq} are the equilibrium length and cross-sectional area, respectively; M_w is the molecular weight; d is the density; K is the force constant; TM is the tensile modulus; TS and TC are the tensile and compressive strength, respectively; ε_T and ε_C are the maximal percentage elongation change at tensile failure, and compressive 'kinking', respectively; ΔH_T and ΔH_C are energy changes from equilibrium value at tensile failure and compressive 'kinking' respectively

[b] Estimated density[43]

[c] X-ray calculated density[29]

A comparison of the mechanical properties of the rigid-rod polymers studied in this work is given in *Table 3*.

CONCLUSIONS

The chain moduli of polymers calculated by the AM1 semi-empirical MO method in this study are shown to be higher than the measured values for two reasons. First, real solid material properties are limited by defects and imperfections, while the calculations are performed on a model of an idealized single polymer chain. This approach does not take into account intermolecular interactions, which are important in determining bulk properties, especially compressive properties. Indeed, solid-state semi-empirical methods are under development[41], and will be used in our continued effort to study the mechanical properties of rigid-rod polymers. Secondly, the semi-empirical method systematically overpredicts bond stiffnesses and moduli as discussed in paper 1 of this series[24].

An analysis of molecular deformation on tension and compression of the rigid-rod polymers offers an insight into tensile and compressive processes at the molecular level. The calculated modulus is non-linear, as has been shown experimentally[26], and is greater in tension than in compression (*Figure 10*). Phenyl rings oriented at a *para* position are easier to deform than heterocyclic moieties in rigid rods, so that their elimination may increase the modulus. In compression, rigid rods tend to bend or 'kink' at the C–C linkage at approximately 2% strain. Also, a critical energy value can be assigned to a compressive or tensile failure, which should be proportional to the force required to cause the failure (cf. *Figure 11*). This allows a relative ordering of polymers by the theoretical tensile and/or compressive strength. An examination of the electron distribution in some of these molecular systems on the application of tensile or compressive strain shows that the *trans* configuration (X vs. Y in *Figure 1*) influences the electron distribution on the application of tensile strain, while the type of the Y atom (O vs. S) affects the π-conjugation on compression.

The theoretical model presented in this study provides definitive information and fresh insights on the compressive and tensile capability of polymer chains, especially useful for comparisons of mechanical properties for a series of related polymers (cf. *Figure 10* and *Table 3*), and for a relative prediction of the properties of PBI polymers that have not yet been synthesized in high molecular weight.

ACKNOWLEDGEMENTS

The authors wish to thank the referee for a very useful critique, and Professors Ronald K. Eby, Robert J. Young and Buckley Crist Jr for fruitful discussions.

REFERENCES

1 Adams, W. W. and Helminiak, T. E. 'Science of Ceramic Chemical Processing', Wiley, New York, 1986, p. 444
2 Adams, W. W. and Eby, R. K. *Mater. Res. Soc. Bull.* 1987, **5**, 22
3 Kwolek, S., US Patent 3 600 356, 1971
4 Kumar, S., Adams, W. W. and Helminiak, T. E. *J. Reinforced Plast. Compos.* 1988, 108
5 Kumar, S. *Int. Encycl. Compos.* 1991, **4**, 51
6 Wolfe, J. F. *Encycl. Polym. Sci. Eng.* 1988, **11**, 601
7 Adams, W. W., Eby, R. K. and McLemore, D. E. (Eds) 'The Materials Science and Engineering of Rigid Rod Polymers', *Mater. Res. Soc. Symp. Proc.* 1989, **134**
8 Farmer, B. L., Wierschke, S. G. and Adams, W. W. *Polymer* 1990, **31**, 1637 and references therein
9 Tashiro, K., Kobayashi, M. and Tadokoro, H. *Macromolecules* 1978, **11**, 908 and references therein
10 Kovar, R. F. and Arnold, F. E. *J. Polym. Sci., Polym. Chem. Edn* 1976, **14**, 2807
11 Hunsaker, M., Fratini, A. V. and Adams, W. W. Report AFWAL-TR-83-4055, 1983
12 Helminiak, T. E., Arnold, F. E. and Benner, C. L. *Polym. Prepr., ACS Polym. Div.* 1975, **16** (2), 659
13 Wolfe, J. F. and Arnold, F. E. *Macromolecules* 1981, **14**, 909
14 Choe, E. W. and Kim, S. N. *Macromolecules* 1981, **14**, 920
15 Wolfe, J. F., Loo, B. H. and Arnold, F. E. *Polym. Prepr., ACS Polym. Div.* 1978, **19** (2), 1
16 Wolfe, J. F., Loo, B. H. and Arnold, F. E. *Macromolecules* 1981, **14**, 915
17 Wellman, M. W., Adams, W. W., Wolff, R. A., Dudis, D. S., Wiff, D. R. and Fratini, A. V. *Macromolecules* 1981, **14**, 935
18 Stewart, J. J. P., MOPAC (Version 5.0), QCPE Program No. 455
19 Stewart, J. J. P. *New Polym. Mater.* 1987, **1**, 53
20 Perkins, P. G. and Stewart, J. J. P. *J. Chem. Soc., Faraday Trans. (II)* 1980, **76**, 520
21 Klei, H. E. and Stewart, J. J. P. *Int. J. Quantum Chem., Quantum Chem. Symp.* 1986, **20**, 529
22 Wiberg, K. G. *Tetrahedron* 1968, **24**, 1083
23 Klunzinger, P. E., Green, K. A., Eby, R. K., Farmer, B. L., Adams, W. W. and Czornyj, G. Preprint, SPE ANTEC, May 1991, Montreal
24 Shoemaker, J. R., Horn, T., Haaland, P. D., Pachter, R. and Adams, W. W. *Polymer* 1992, **33**, 3351

25 Ang, C. P. P., Ph.D. Thesis, University of Manchester, 1991
26 Jiang, H., Eby, R. K., Adams, W. W. and Lenhert, G. in 'The Materials Science and Engineering of Rigid Rod Polymers', *Mater. Res. Soc. Symp. Proc.* 1989, **134**, 341
27 Wierschke, S. G., Report AFWAL-TR-88-420, 1988
28 Young, R. J. 'Rigid Rod Polymer Fibers and Composites', Specialty Polymers, 1990, Baltimore, MD
29 Fratini, A. V., Lenhert, P. G., Resch, T. J. and Adams, W. W. in 'The Materials Science and Engineering of Rigid Rod Polymers', *Mater. Res. Soc. Symp. Proc.* 1989, **134**, 431
30 Staudinger, H. *Zweiter Teil (B)* 1932, **II 4**, 263
31 Karasawa, N., Dasgupta, S. and Goddard, W. A. *J. Phys. Chem.* 1991, **95**, 2260
32 Shoemaker, J. R., M.Sc. Thesis, Air Force Institute of Technology, 1991
33 Wool, R. P. and Bretzlaff, R. S. *J. Polym. Sci. (B), Polym. Phys. Edn. 1986*, **24**, 1039
34 Martin, D. C., Ph.D. Thesis, University of Massachusetts, 1991
35 Allen, S. R., Filippov, A. G., Farris, R. J., Thomas, E. L., Wong, C. P., Berry, G. C. and Chenevey, E. C. *Macromolecules* 1981, **14**, 1135
36 Rao, D. N., Swiatkiecz, J., Chopra, P., Ghoshal, S. K. and Prasad, P. N. *Appl. Phys. Lett.* 1986, **48**, 1187
37 Garito, A. F., Wong, K. Y., Cai, Y. M., Man, H. T. and Zamani, O. 'Molecular and Polymeric Optoelectronic Materials: Fundamentals and Applications' (Ed. G. Khanarian), *Proc. SPIE* 1986, **682**, 2
38 Goldfarb, I. J., Reale, H., Wierschke, S. and Medrano, J. in 'The Materials Science and Engineering of Rigid Rod Polymers', *Mater. Res. Soc. Symp. Proc.* 1989, **134**, 609
39 Tompson, R. D. *Prog. Org. Chem.* 1976, **12**,
40 Paolini, J. H. *J. Comp. Chem.* 1990, **11**, 1160
41 Stewart, J. J. P., MOSOL, QCPE Program No. 495
42 Lenhert, P. G. and Adams, W. W. in 'The Materials Science and Engineering of Rigid Rod Polymers', *Mater. Res. Soc. Symp. Proc.* 1989, **134**, 329
43 Adams, W. W., Kumar, S. and Fratini, A. V. personal communication, 1988